

RSC Advances



This is an *Accepted Manuscript*, which has been through the Royal Society of Chemistry peer review process and has been accepted for publication.

Accepted Manuscripts are published online shortly after acceptance, before technical editing, formatting and proof reading. Using this free service, authors can make their results available to the community, in citable form, before we publish the edited article. This *Accepted Manuscript* will be replaced by the edited, formatted and paginated article as soon as this is available.

You can find more information about *Accepted Manuscripts* in the [Information for Authors](#).

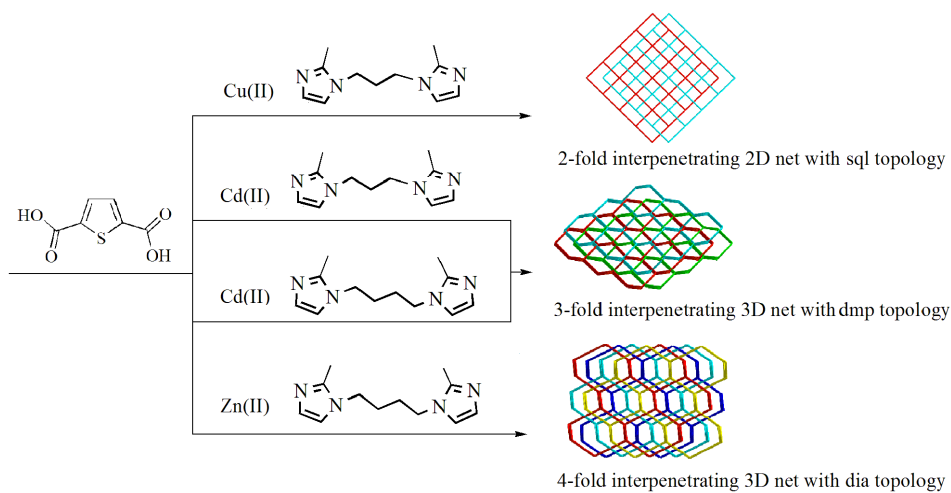
Please note that technical editing may introduce minor changes to the text and/or graphics, which may alter content. The journal's standard [Terms & Conditions](#) and the [Ethical guidelines](#) still apply. In no event shall the Royal Society of Chemistry be held responsible for any errors or omissions in this *Accepted Manuscript* or any consequences arising from the use of any information it contains.

Graphical Abstract:

Title: Four d^{10} metal coordination polymers based on bis(2-methyl imidazole) spacers: syntheses, interpenetrating structures and photoluminescence properties

Key Topic:

Combining 2,5-thiophenedicarboxylate and bis(2-methyl imidazole) mixed ligands, four d^{10} metal CPs with 4-connected 2-fold interpenetrating **sql**, 3-fold interpenetrating **dmp** and 4-fold interpenetrating **dia** networks have been constructed and characterized.



Four d¹⁰ metal coordination polymers based on bis(2-methyl imidazole) spacers: syntheses, interpenetrating structures and photoluminescence properties

Li-Ping Xue,^a Xin-Hong Chang,^a Lu-Fang Ma,^{*a} and Li-Ya Wang^{*a,b}

5 Received (in XXX, XXX) Xth XXXXXXXXXX 2014, Accepted Xth XXXXXXXXXX 2014

First published on the web Xth XXXXXXXXXX 2014

DOI:

Two bis(2-methyl imidazole) ligands have been applied to assemble four interpenetrating coordination polymers with formula [Cu₂Br₂(bip)]_n (**1**), [Cd(tdc)(bip)]_n (**2**), [Cd(tdc)(bib)]_n (**3**),
10 and [Zn(tdc)(bib)]_n (**4**) (tdc = 2,5-thiophenedicarboxylate anion, bip = 1,3-bis-(imidazol-2-methyl)propane and bib = 1,4-bis(imidazol-2-methyl)butane) under hydrothermal conditions. Structural analyses reveal that complex **1** exhibits a 2-fold interpenetrating 2D net with **sql** topology, whereas complexes **2** and **3** feature 3-fold interpenetrating 3D net with **dmp** topology. Complex **4** displays a [2 + 2] 4-fold interpenetrating 3D net with **dia** topology. These results
15 provide some insight into central metal ions, anionic ligands and bis(2-methyl imidazole) ligands geometry-driven assembly of various interpenetrating CPs. Solid-state properties for these crystalline materials, such as thermal stabilities, powder X-ray diffraction have been investigated. Moreover, photoluminescence behaviors of complexes **1–4** are also investigated.

Introduction

20 Coordination polymers (CPs) are an important class of functional materials constructed from metal ions and organic ligands with elegant topologies and potential functionality.¹ Because the final structures of CPs are often rely on many synthetic parameters, currently, it is still a great challenge to
25 design and construct a target structure with the specific net topology. Accompanied by the rapid development of CPs, topological control has served as an effective approach to guide the synthesis of functional CPs with desirable properties.² According to previous reports, some 3–8 and even
30 higher-connected uninodal network have been discovered.³ Among them, nodes of 4-connectivity, possessing zeolite analog structures, capture much attention owing to their inherent interest in crystal engineering.⁴ During the assembly process of 4-connected CPs, it has been observed that the
35 introduction of long N,N'-donor ligands usually lead to interpenetrating networks.⁵ As the most investigated type of entanglement, the origin of interpenetration of CPs has been contribution to the presence of large free voids in a single framework and mutual interpenetration of the networks
40 usually reduces potential porosity. Although there has been a growing trend in using polycarboxylate ligands with flexible N,N'-donor ancillary ligands to construct intriguing interpenetrating architectures, the factors that influence the resulting degree of interpenetration still remain unknown to
45 date.⁶ Therefore, a survey about interpenetration derived from modulation of the central metal ions and linkages is still of great challenge and focus.

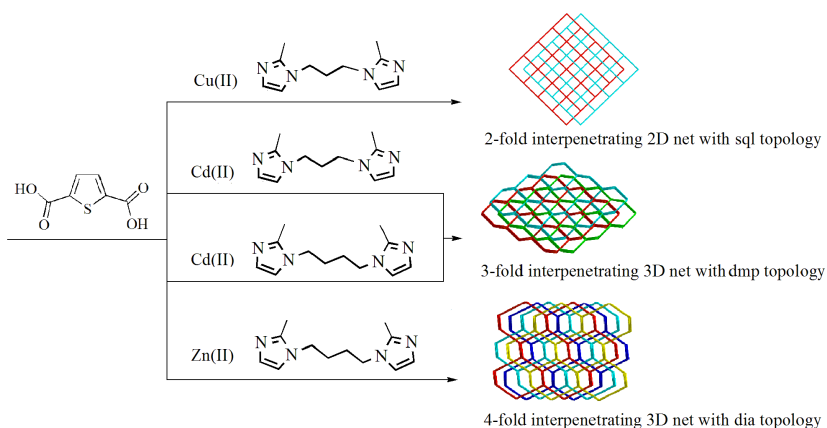
In the self-assembly process of interpenetrating structures, flexible N,N'-donor ligands are able to twist and rotate freely
50 to adopt a suitable conformation, which are more prone to having larger voids. Usually, the larger voids in the motif, the

more likely interpenetration will be generated. In contrast to those flexible bis(imidazole) ligands commonly used in the literatures,⁷ 1,3-bis-(imidazol-2-methyl)propane (bip) and 1,4-bis(2-methyl-imidazol-1-yl)butane (bib) ligands bearing a pair of methyl groups are good candidates for the formation of interpenetrating CPs.⁸ The methyl on the imidazole ring can greatly enhance the electron donating ability of the ligand, and maybe create steric hindrance to modulate the topologies and interpenetrating dimensions. In addition, CPs based on 2,5-thiophenedicarboxylic acid (H₂tdc) and N,N'-donor ligands have received increasing attention due to their interesting topologies and improved luminescence intensity.⁹ However, the combination of H₂tdc and ancillary
65 flexible bis(2-methyl imidazole) ligands are rather limited. By introducing bis(2-methyl imidazole) ligands into the H₂tdc synthesis system, we could study the effects of the central metal ions, anionic ligands and bis(2-methyl imidazole) ligands geometry-driven assembly of interpenetrating CPs and
70 reveal how bis(2-methyl imidazole) ligands together with H₂tdc behave to match the central metal ions to generate different interpenetrating networks. In this contribution, we performed hydrothermal reactions of H₂tdc and ancillary bis(2-methyl imidazole) ligands with d¹⁰ transition-metal ions.
75 Four interpenetrating CPs with different structures and topologies, namely [Cu₂Br₂(bip)]_n (**1**), [Cd(tdc)(bip)]_n (**2**), [Cd(tdc)(bib)]_n (**3**), and [Zn(tdc)(bib)]_n (**4**), have been obtained. The effect of central metal ions, anionic ligands and bis(2-methyl imidazole) ligands on the ultimate structures will
80 be represented and discussed. The thermal stabilities and solid-state photoluminescence properties of these CPs have also been investigated below in detail.

Experimental section

5

10



Scheme 1 Synthetic procedures of complexes **1–4**.

Materials and methods

The ligand bib and bip were prepared similarly as described in the literature procedure.¹⁰ Other reagents were obtained commercially and used without further purification. The IR spectra were recorded as KBr pellets on a Nicolet Avatar-360 spectrometer in the range of 4000 to 400 cm⁻¹. Elemental analyses for C, H, and N were carried out on a Flash 2000 elemental analyzer. Powder X-ray diffraction (PXRD) measurements were performed on a Bruker D8-ADVANCE X-ray diffractometer with Cu K α radiation ($\lambda = 1.5418 \text{ \AA}$). Thermogravimetric analyses (TGA) were carried out on a SDTQ600 thermogravimetric analyzer. A platinum pan was used for heating the sample with a heating rate of 10 °C/min under air atmosphere. Fluorescence measurements were recorded with a Hitachi F4500 fluorescence spectrophotometer.

[Cu₂Br₂(bip)]_n (**1**)

A mixture of H₂tdc (17.2 mg, 0.1 mmol), CuBr₂·2H₂O (22.3 mg, 0.1 mmol), bip (40.8 mg, 0.2 mmol), and 10 mL deionized water was sealed in a 25 mL Teflon-lined stainless

steel vessel and heated at 120 °C for 5 days under autogenous pressure, followed by cooling to room temperature at a rate of 5 °C h⁻¹. Yellow prismatic crystals of **1** were collected (yield: 15% based on copper). Elemental analysis calcd (%) for C₁₁H₁₆N₄Br₂Cu₂: C, 26.87; H, 3.26; N, 11.40. Found: C, 26.56; H, 3.31; N, 11.51. IR (cm⁻¹): 3113(w), 2924(w), 1600(w), 1538(m), 1500(m), 1417(m), 1373(w), 1277(m), 1154(m), 1126(w), 1091(w), 998(m), 942(w), 844(m), 743(s), 673(m).

[Cd(tdc)(bip)]_n (**2**)

A mixture of H₂tdc (17.2 mg, 0.1 mmol), Cd(OAc)₂·2H₂O (26.7 mg, 0.1 mmol), bip (20.4 mg, 0.1 mmol), and 10 mL deionized water was sealed in a 25 mL Teflon-lined stainless steel vessel and heated at 120 °C for 5 days under autogenous pressure, followed by cooling to room temperature at a rate of 5 °C h⁻¹. Yellow prismatic crystals of **2** were collected (yield: 35% based on cadmium). Elemental analysis calcd (%) for C₁₇H₁₈N₄O₄SCd: C, 41.91; H, 3.70; N, 11.50. Found: C, 41.89; H, 3.73; N, 11.51. IR (cm⁻¹): 3112(m), 2928(w), 1536(m),

Table 1 Crystal data and structure refinements for **1–4**

Complex	1	2	3	4
Formula	C ₁₁ H ₁₆ N ₄ Br ₂ Cu ₂	C ₁₇ H ₁₈ N ₄ O ₄ SCd	C ₁₉ H ₁₈ N ₃ O ₄ SCd	C ₁₈ H ₂₀ N ₄ O ₄ SZn
<i>M_r</i>	491.18	486.81	496.82	453.81
Crystal system	Orthorhombic	Orthorhombic	Orthorhombic	Monoclinic
Space group	<i>Pnn2</i>	<i>Pna2(1)</i>	<i>Pna2(1)</i>	<i>P2(1)/n</i>
<i>a</i> (Å)	9.568(3)	9.2703(14)	9.4781(10)	9.4933(12)
<i>b</i> (Å)	17.673(6)	13.966(2)	13.8347(14)	19.380(2)
<i>c</i> (Å)	9.560(3)	14.650(2)	15.4666(16)	11.4845(14)
β (°)	90	90	90	94.559(2)
<i>V</i> (Å ³)	1616.5(9)	1896.8(5)	2028.1(4)	2106.2(5)
<i>Z</i>	4	4	4	4
ρ (g cm ⁻³)	2.018	1.705	1.627	1.431
μ (mm ⁻¹)	7.566	1.292	1.209	1.295
<i>F</i> (000)	952	976	996	936
GOF (<i>F</i> ²)	1.014	1.072	1.026	1.025
<i>R</i> ₁ ^a [<i>I</i> > 2 σ (<i>I</i>)]	0.0265	0.0302	0.0244	0.0326
<i>wR</i> ₂ ^b [<i>I</i> > 2 σ (<i>I</i>)]	0.0513	0.0556	0.0602	0.0810

$${}^a R_1 = \sum \|F_o| - |F_c|\| / \sum |F_o|, {}^b wR_2 = \{ \sum [w(F_o^2 - F_c^2)^2] / \sum [w(F_o^2)^2] \}^{1/2}$$

1509(m), 1423(s), 1349(s), 1270(m), 1154(m), 1127(w),
1090(w), 999(m), 942(w), 859(w), 844(w), 816(m), 797(m),
754(m), 745(s), 674(s).

[Cd(tdc)(bip)]_n (**3**)

5 The synthesis of **3** was similar to that of **2**, but with bip (21.8 mg, 0.1 mmol) in place of bip. Yellow block crystals of **3** were obtained (yield: 36% based on cadmium). Elemental analysis calcd (%) for C₁₉H₁₈N₃O₄SCd: C, 45.89; H, 3.62; N, 8.45. Found: C, 45.86; H, 3.69; N, 8.49. IR (cm⁻¹): 3114(m),
10 2948(w), 1538(m), 1505(m), 1421(s), 1357(s), 1273(m), 1154(m), 1128(w), 1089(w), 999(m), 943(w), 858(w), 845(w), 817(m), 795(m), 753(m), 744(s), 674(s).

[Zn(tdc)(bip)]_n (**4**)

The synthesis of **4** was similar to that of **3**, but with
15 Zn(OAc)₂·2H₂O (22.0 mg, 0.1 mmol) in place of Cd(OAc)₂·2H₂O. Colorless block crystals of **4** were obtained (yield: 26% based on zinc). Elemental analysis calcd (%) for C₁₈H₂₀N₄O₄SZn: C, 47.60; H, 4.41; N, 12.34. Found: C, 47.56; H, 4.43; N, 12.45. IR (cm⁻¹): 3124(w), 2935(w), 1627(s),
20 1531(m), 1507(w), 1463(m), 1345(vs), 1327(m), 1279(m), 1202(w), 1156(m), 1119(m), 1011(m), 909(w), 854(w), 835(w), 809(s), 765(vs), 734(w), 686(w), 666(m).

X-ray crystallography

The crystal structure data of **1–4** were collected on Bruker
25 SMART APEX II CCD diffractometer equipped with a graphite-monochromated Mo Kα (λ = 0.71073 Å) radiation using an ω scan mode at 293 K. An empirical absorption

correction was applied using the SADABS program.¹¹ The structures were solved by direct methods and refined by full-matrix least-squares on *F*² using the SHELXL-97 program package.¹² All non-hydrogen atoms were refined with anisotropic displacement parameters. A summary of the crystallographic data of **1–4** is listed in Table 1. Selected bond lengths and angles for **1–4** were listed in Tables S1.†

35 Results and discussions

Syntheses

By using bip and bib as the auxiliary ligands, complexes **1–4** were successfully synthesized under hydrothermal conditions. Complex **1** contains Cu(I) bromine cluster, presumably owing
40 to an in situ reduction of Cu(II) to Cu(I) by ligand bip. Using other copper sources as starting materials, only blue precipitate was obtained. Moreover, we did not successfully obtain **1** in the absence of H₂tdc ligand, although H₂tdc was not included in the final product. Complexes **2–4** were
45 obtained when the molar ratio of metal/H₂tdc/bip or bib = 1 : 1 : 1. Despite our efforts to grow single-crystals based on bip, H₂tdc and different zinc sources in the same synthetic condition of **2**, only microcrystalline precipitate unsuitable for study of X-ray diffraction was obtained.

50 Structural description of [Cu₂Br₂(bip)]_n (**1**)

Single-crystal X-ray diffraction reveals that **1** crystallizes in the orthorhombic system with *Pnn2* space group. Complex **1** exhibits a 2-fold interpenetrating 2D net with a **sql** topology

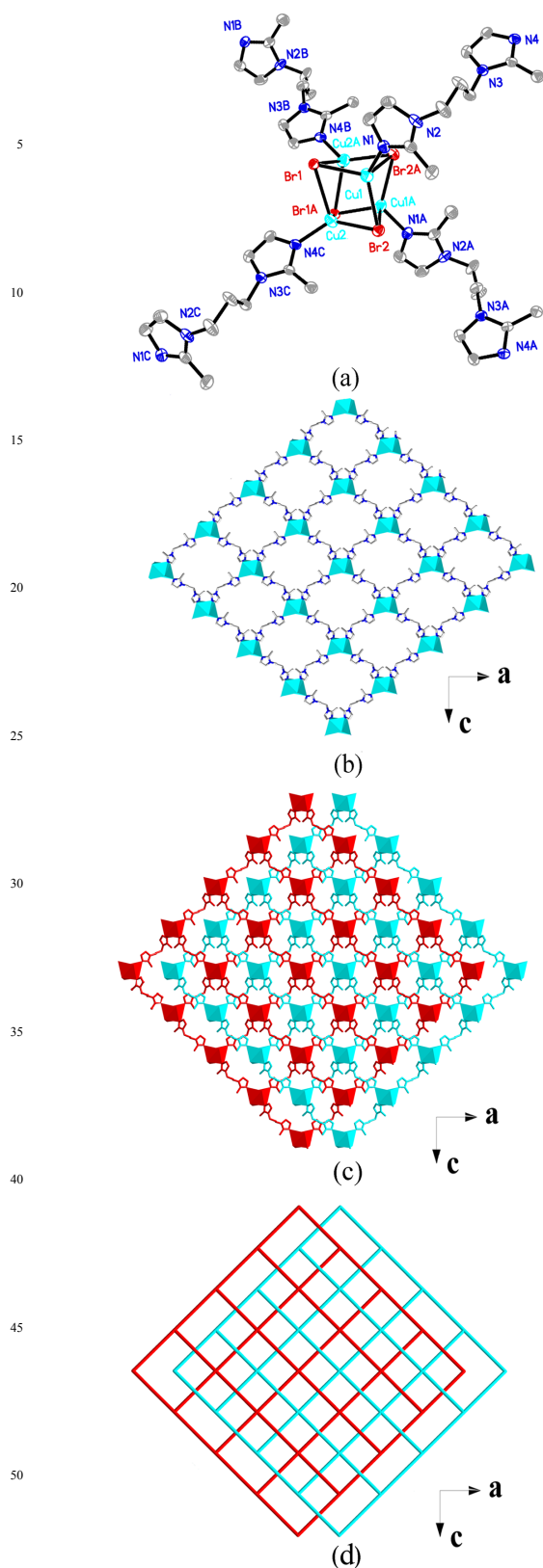


Fig. 1 (a) Molecular structure of **1** containing a cubane $[\text{Cu}_4\text{Br}_4]$ cluster. Symmetry codes: (A) $2 - x, 2 - y, z$; (B) $1 - x, 2 - y, z - 1$; (C) $1 + x, y, z - 1$. (b) A single 2D layer structure of **1**. (c) View of the 2-fold interpenetrating 3D framework of **1**. (d) Topological representation of the 2-fold interpenetration in **1**.

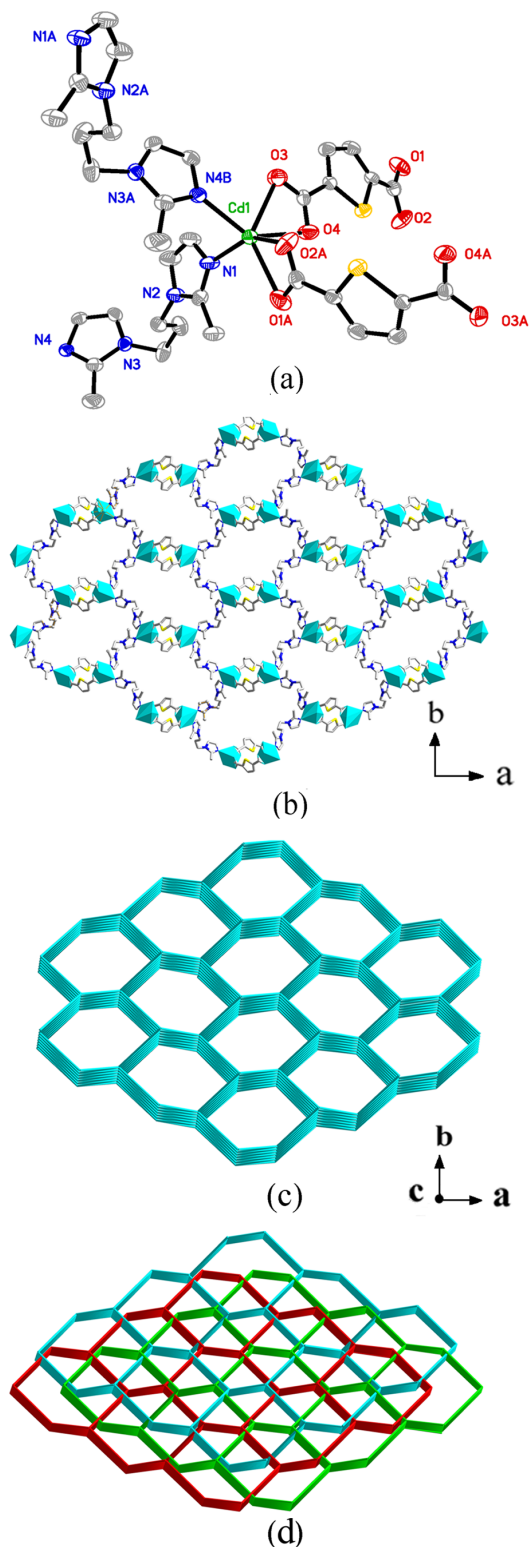
and is constructed from distorted Cu_4Br_4 tetrameric skeletal cores as secondary building units. As shown in Fig. 1a, the repeating tetrameric skeletal core is composed of four copper(I) ions and four Br^- anions

connected alternately to each other in a distorted cubane-like arrangement.

Each copper(I) ion is four coordinated, surrounded by three bromine anions and one nitrogen atom from bip to furnish a distorted NBr_3 tetrahedral geometry.

The Cu–Br distances range from 2.4251(11) to 2.7192(10) Å (average value 2.5886 (8) Å) and Cu–N distance is 1.992(4) Å, similar to those reported in similar complexes.¹³

Moreover, the distances of $\text{Cu}\cdots\text{Cu}$ are 2.7645(11), 2.8299(11) and 2.8625(16) Å in the Cu_4Br_4 cubane cluster, which are shorter than or comparable to the sum of the van der Waals radii of copper(I) (2.80 Å), and thus imply significant $\text{Cu}\cdots\text{Cu}$ bonding interactions. In complex **1**, each bip ligand adopting the *anti-gauche* conformation connect two adjacent Cu_4Br_4 clusters. From the view of topology, these Cu_4Br_4 clusters act as four-connecting nodes that are jointed to each other *via* four bip ligands, affording a 4^4-sql



and is constructed from distorted Cu_4Br_4 tetrameric skeletal cores as secondary building units. As shown in Fig. 1a, the repeating tetrameric skeletal core is composed of four copper(I) ions and four Br^- anions connected alternately to each other in a distorted cubane-like arrangement. Each copper(I) ion is four coordinated, surrounded by three bromine anions and one nitrogen atom from bip to furnish a distorted NBr_3 tetrahedral geometry. The Cu–Br distances range from 2.4251(11) to 2.7192(10) Å (average value 2.5886 (8) Å) and Cu–N distance is 1.992(4) Å, similar to those reported in similar complexes.¹³ Moreover, the distances of $\text{Cu}\cdots\text{Cu}$ are 2.7645(11), 2.8299(11) and 2.8625(16) Å in the Cu_4Br_4 cubane cluster, which are shorter than or comparable to the sum of the van der Waals radii of copper(I) (2.80 Å), and thus imply significant $\text{Cu}\cdots\text{Cu}$ bonding interactions. In complex **1**, each bip ligand adopting the *anti-gauche* conformation connect two adjacent Cu_4Br_4 clusters. From the view of topology, these Cu_4Br_4 clusters act as four-connecting nodes that are jointed to each other *via* four bip ligands, affording a 4^4-sql

2D network along the *ac* plane and the rectangular window of the 2D motif has the dimension of ca. 15 Å × 14 Å (Fig. 1b). Moreover, each 2D layer has enough “empty” space to allow another 2D layer to interpenetrate to form a two-fold parallel interwoven net (Fig. 1c and Fig. 1d). Calculations using PLATON based on the crystal structure show that the total solvent-accessible volume comprises 9.4% (1616.5 Å³) of the crystal volume.

Structural description of [Cd(tdc)(bip)]_n (2) and [Cd(tdc)(bib)]_n (3)

Single crystal X-ray analysis reveals that complexes **2** and **3** are isostructural. For the convenience of depiction, the structure of complex **2** is described as a representative example in detail. Crystallographic analysis shows that **2** crystallizes in the *Pna*2(1) space group and exhibits a 3-fold interpenetrating 3D net with a **dmp** topology. The asymmetric unit consists of one independent Cd(II) ion, one tdc²⁻ anion and one bip ligand. The coordination environment around the Cd(II) ion is best portrayed as a distorted [CdN₂O₄] octahedral geometry, finished by four carboxylate oxygen atoms of two tdc²⁻ anions and two imidazol nitrogen atoms from two bip ligands (Fig. 2a). The bond lengths of Cd–N are 2.239(5) (Cd–N1) and 2.267(4) Å (Cd–N4), while Cd–O bond lengths vary from 2.255(4) to 2.504(5) Å, which are in the normal range. In **2**, Each tdc²⁻ anion serves as a μ₂ bridge linking two adjacent Cd(II) ions by adopting bidentate-chelating coordination mode to give rise to a 1D zigzag chain along *c* axis. And each flexible bip ligand is ligated to two Cd(II) ions with two terminal imidazol groups assuming the *anti-gauche* conformation to extend the 1D zigzag chain to a 3D coordination network (Fig. 2b). From the topological view, if each Cd(II) ion is considered as a 4-connected node, tdc²⁻ anions and bip ligands can be simplified as linear connectors, then an uninodal 4-connected **dmp** net with (6⁵.8) topology was observed in this structure (Fig. 2c). The large void produced in this connectivity is filled by 3-fold interpenetration (Fig. 2d). According to Reticular Chemistry Structure Resource (RCSR) database, many CPs with 4-connected **dmp** topology have been obtained in recent studies, however, the number of 3-fold interpenetrating CPs with the topology is still limited.¹⁴

Fig. 2 (a) Coordination environment of Cd(II) ion in **2**. Symmetry codes: (A) 1 – *x*, 1 – *y*, 0.5 + *z*; (B) –0.5 – *x*, 0.5 + *y*, 0.5 + *z*. (b) A single 3D framework of **2**. (c) View of the 4-connected 3D **dmp** topology. (d) Schematic view of the 3-fold interpenetration in **2**.

Structural description of [Zn(tdc)(bib)]_n (4)

When Zn(II) was used instead of Cd(II) in the synthesis of **3**, complex **4** was obtained. Single crystal X-ray structural analysis reveals that **4** crystallizes in the monoclinic space group *P*2(1)/*n* and exhibits a 4-fold interpenetrating 3D net with **dia** topology. As shown in Fig. 3a, the asymmetric unit is composed of one Zn(II) ion, one tdc²⁻ anion, and one bib ligand (Fig. 3a). Each Zn(II) ion is four-coordinated with

distorted tetrahedral geometry and defined by two carboxylate oxygen atoms from two tdc²⁻ anions (Zn–O bond lengths are 1.9375(18), and 1.9805(19) Å) and two N-atoms donor from two bib ligands (Zn–N bond lengths are 2.030(2), and 1.987(2) Å). Both Zn–O and Zn–N bond lengths are well-matched to those observed in similar complexes. It is noted that the maximum and minimum bond angles for Zn are 126.78(9) and 99.42(9)°, respectively, with an average value of 108.95(8)°, which slightly deviates from the angle of 109.47 ° in a perfect tetrahedron. Each tdc²⁻ anion, unlike complex **2**, adopts in a bis-monodentate coordination fashion and flexible bib ligand assumes an *anti-anti-anti* conformation.

Six tdc²⁻ anions and six bib connected ten tetrahedral nodes of Zn(II) ions to form a fundamental [Zn₁₀(bib)₆(tdc)₆] adamantanoid cage containing four cyclohexane-like windows, each in a chair conformation (Fig. 3b). The Zn···Zn distances across bib and tdc²⁻ anions are 13.8320 Å and 10.6672 Å, respectively. The tdc²⁻ anions alternately bridge two adjacent Zn(II) ions in a bis-monodentate coordination fashion to generate a chain, which are connected by the bib ligand to form a 3D framework containing adamantanoid-like subunits. Topologically, Zn(II) ions could be regarded as 4-connected nodes, the bib ligands and tdc²⁻ anions serve as linear linkers. As a result, the structure of **4** represents an uninodal 3D 4-connected **dia** (6⁶) topology (Fig. 3c). The single 3D network consists of large windows, which are filled via mutual interpenetration of four independent equivalent networks (Fig. 3d). Interestingly, the mode of interpenetration is different from the normal mode and may be described as two sets of normal 2-fold nets, that is, an unusual [2 + 2] mode of interpenetration (Fig. 3e and Fig. 3f). Meanwhile, **4** is also regarded as a roto-translational [2 + 2] interpenetrating diamondoid system (the class IIIa in RSCR notation). To our knowledge, among those unusual interpenetrating examples, the roto-translational nets are rare.¹⁵ Such 4-fold interpenetration modes can minimize the big void cavities of the diamondoid cages and the whole accessible solvent volumes is ~5.2% (2106.2 Å³) per unit cell volume by calculated using PLATON.

Structural comparison of complexes 1–4

As we know, central metal ions, anionic ligands and ancillary N-donor ligands have a remarkable effect on the construction of CPs. Herein, we have prepared four 4-connected CPs by employing three types of d¹⁰ metal salts, H₂tdc and two types of flexible bis(2-methyl imidazole) spacers to investigate their distinct effects on structural diversity and interpenetrating variation. The tetranuclear clusters in **1** and metal ions in complexes **2–4** are coordinated by four bridging ligands to serve as 4-connected nodes, finally resulting in typical 4-connected networks.

As far as **1** and **2**, **3** and **4** are concerned, respectively, the

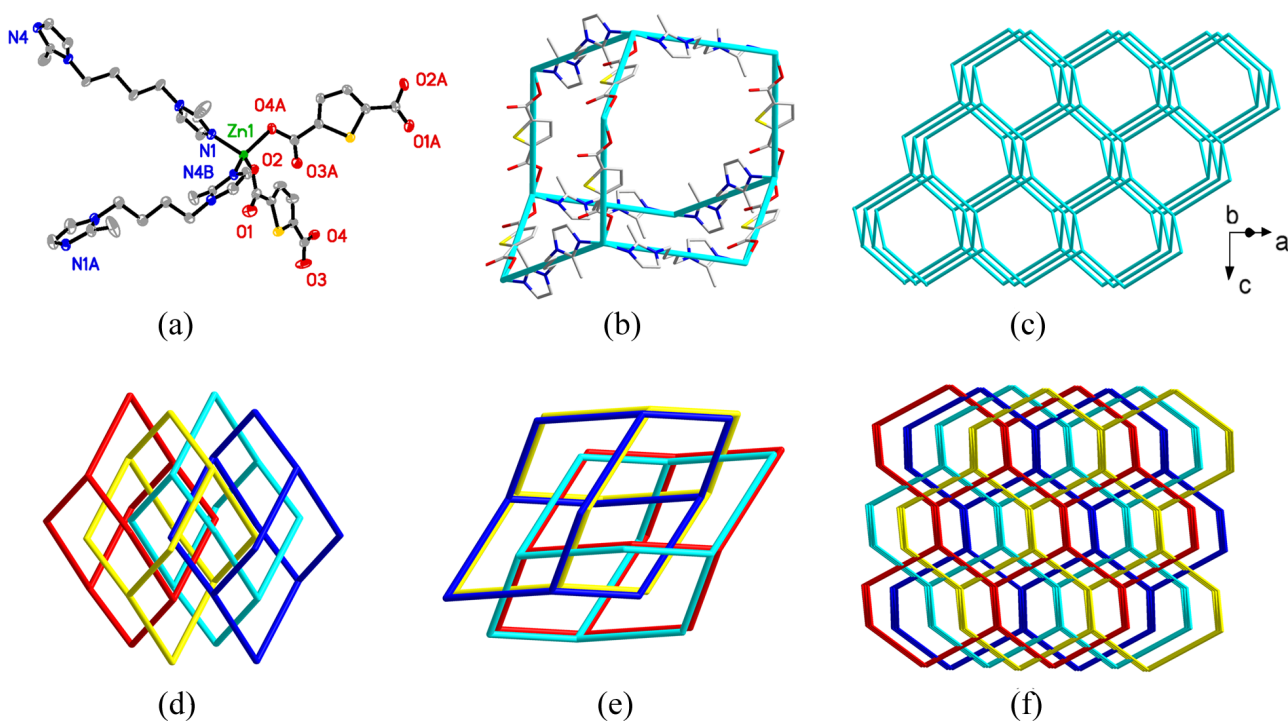


Fig. 3 (a) Coordination environment of Zn(II) ions in **4**. Symmetry codes: Symmetry code: (A) $0.5 + x, 1.5 - y, 0.5 + z$. (B) $0.5 + x, 0.5 - y, z - 0.5$. (b) View of a single diamond motif in **4**. (c) Schematic view of a single 3D diamond framework. (d) Schematic representation of the 4-fold interpenetrating adamantanoid cages. (e) Schematic representation of [2+2] fold interpenetration. (f) Schematic representation of the 4-fold interpenetrating 3D diamond framework.

same ligand combination but different metal ions are used. In **1**, Cu(I) ions were *in situ* obtained via hydrothermal reactions of CuBr_2 with bip spacers and the resulting Cu(I) ions with Br^- anions spontaneously assemble into Cu_4Br_4 tetranuclear clusters. The clusters are further linked by bip spacers to generate the 2D layer, which house larger space to allow the interpenetration of another 2D layer, affording a 2-fold interpenetrating **sql** net. By contrast, Cd(II) ions, tdc^{2-} anions together with bip spacers are incorporated in **2** and a 3-fold interpenetrating **dmp** net is formed. Obviously, synergistic metal centers and anionic ligands effects led to the structural differences. Structural differences of **3** and **4** can be attributed to the changes of metal ions. Since the radii of Cd(II) ions are larger than Zn(II) ions, the coordination numbers of the Cd(II) ions are higher than Zn(II) ions. In the assembly process, tdc^{2-} anions together with flexible bip bridging spacers meet the requirement of coordination geometries of Zn(II) and Cd(II) ions to form **dmp** and **dia** nets, respectively. Furthermore, the void space in **3** and **4** is relatively large and facilitates to generate rare 3-fold or 4-fold interpenetrating net. Finally, structural similarity of **2** and **3** exhibits that the subtle difference of auxiliary bis(2-methyl imidazole) ligands are not sufficient in determining the final structures, which also indicates metal centers and anionic ligands should be the key factor in the assembly of **2** and **3**.

30 Powder X-ray diffraction and thermogravimetric analyses

Powder X-ray diffraction experiments were carried out for the bulky samples **1–4**. The patterns for the as-synthesized bulky samples closely match the simulated ones from the single-

crystal structure analysis, which are indicative of the high purity of the synthesized samples (Fig. S1, ESI).† The difference in reflection intensities between the simulated and experimental patterns may be owing to the variation in preferred orientation of the powder samples during the collection of the PXRD data. To further evaluate the stability of **1–4**, thermal behaviors were investigated under N_2 atmosphere with a heating rate of $10\text{ }^\circ\text{C}/\text{min}$ (Fig. S2, ESI).† No weight losses are observed in the temperature ranges of 30–336 for **1**, 30–275 for **2**, 30–272 for **3** and 30–220 $^\circ\text{C}$ for **4**. They are in good agreement with the crystal structures of the four complexes, in which no solvents are included. Above these temperatures, the samples suffered an abrupt weight loss, indicating the decomposition of the organic components and the collapse of the networks.

Photoluminescence properties

Due to insoluble in common solvents, the fluorescence spectra of complexes **1–4** were measured in solid state at room temperature (Fig. S3, ESI).† As well known, Cu(I) halide-based complexes usually exhibit excellent luminescence properties. Complex **1** is yellow powder under ambient light and can emit intense orange light under UV irradiation. The solid of **1**, when excited by 368 nm, exhibited intense orange fluorescence with emission maxima at 566 nm. On the basis of the studies on the luminescence of copper(I) halides, the emission should be attributed primarily to a combination of bromine-to-copper charge transfer and copper-centered transition from $3d^{10}$ to $3d^94s$ and from $3d^{10}$ to $3d^94p$ in copper(I) centers.¹⁶ The pure ligands display luminescence

emission bands at 350 nm ($\lambda_{\text{ex}} = 300$ nm) for H₂tdc, 410 nm ($\lambda_{\text{ex}} = 300$ nm) for bip, and 465 nm ($\lambda_{\text{ex}} = 280$ nm) for bib.¹⁷ It can be assumed that these peaks derive from the $\pi^* \rightarrow n$ or $\pi^* \rightarrow \pi$ transitions. The emission spectra for complexes **2–4** exhibit emission peaks at 478 nm ($\lambda_{\text{ex}} = 326$ nm), 435 nm ($\lambda_{\text{ex}} = 330$ nm), and 500 nm ($\lambda_{\text{ex}} = 314$ nm), respectively (Fig. 5b). According to the literature, fluorescent emission of polycarboxylates generated from the $\pi^* \rightarrow n$ transition is very weak compared with the $\pi^* \rightarrow \pi$ transition of the N,N'-donor ligands, so polycarboxylates almost have no significant contribution to the fluorescent emission of the as-synthesized complexes.¹⁸ Moreover, Cd(II) ions and Zn(II) ions are difficult to oxidize or reduce due to their d¹⁰ configuration. Therefore, fluorescent emission bands of **2–4** may be assigned to intraligand $\pi^* \rightarrow \pi$ transitions of the neutral ligands because these peaks are similar to the free bip or bib ligand, respectively.

Conclusions

In summary, four 4-connected interpenetrating CPs have been successfully constructed *via* the self-assembly of two structurally related flexible bis(2-methyl imidazole) ligands with d¹⁰ metal salts and H₂tdc. Structures and topologies of these compounds, except for isostructural **2** and **3**, are distinct from one another. Structural diversities of the complexes indicate that central metal ions and anionic ligands have significant effects on the resultant interpenetrating structures. The results of the present study suggest that the combination of suitable metal salts and anionic ligands with flexible bis(2-methyl imidazole) might form coordination polymers with interpenetrating structures.

Acknowledgements

This work was supported by the National Natural Science Foundation of China (21401097, 21371089 and 21271098), and sponsored by Program for New Century Excellent Talents in University (NCET-11-0947), Innovation Scientists and Technicians Troop Construction Projects of Henan Province (134100510011) and supported by Program for Innovative Research Team (in Science and Technology) in University of Henan Province.

Notes and references

^aCollege of Chemistry and Chemical Engineering, Luoyang Normal University, Luoyang, Henan 471022, P. R. China

^bCollege of Chemistry and Pharmaceutical Engineering, Nanyang Normal University, Nanyang 473061, P. R. China.

^cE-mail: mazhuxp@126.com, wlyya@lynu.edu.cn

†Electronic Supplementary Information (ESI) available: CCDC: 995971-995974 for complexes **1–4**. For ESI and crystallographic data in CIF or other electronic format See DOI:

(a) M. Li, D. Li, M. O'Keeffe and O. M. Yaghi, *Chem. Rev.*, 2014, **114**, 1343; (b) T. R. Cook, Y. R. Zheng and P. J. Stang, *Chem. Rev.*, 2013, **113**, 734; (c) D. Zhao, D. J. Timmons, D. Yuan and H.-C. Zhou, *Acc. Chem. Res.*, 2011, **44**, 123; (d) O. K. Farha and J. T. Hupp, *Acc. Chem. Res.*, 2010, **43**, 1166; (e) S. Qiu and G. Zhu, *Coord. Chem. Rev.*, 2009, **253**, 2891.

- (a) H. X. Deng, C. J. Doonan, H. Furukawa, R. B. Ferreira, J. Towne, C. B. Knobler, B. Wang and O. M. Yaghi, *Science*, 2010, **327**, 846; (b) X.-J. Li, F.-L. Jiang, M.-Y. Wu, S.-Q. Zhang, Y.-F. Zhou and M.-C. Hong, *Inorg. Chem.*, 2012, **51**, 4116; (c) Z.-M. Zhang, S. Yao, Y.-G. Li, Y. Lu, Z.-M. Su and E.-B. Wang, *J. Am. Chem. Soc.*, 2009, **131**, 14600; (d) Y. Qi, Y.-X. Che, S. R. Batten and J.-M. Zheng, *CrystEngComm*, 2008, **10**, 1027; (e) W.-C. Song, Q. Pan, P.-C. Song, Q. Zhao, Y.-F. Zeng, T.-L. Hu and X.-H. Bu, *Chem. Commun.*, 2010, **46**, 4890; (f) D.-S. Li, X.-J. Ke, J. Zhao, M. Du, K. Zou, Q.-F. He and C. Li, *CrystEngComm*, 2011, **13**, 3355; (g) A.-L. Cheng, Y. Ma, J.-Y. Zhang and E.-Q. Gao, *Dalton Trans.*, 2008, 1993; (h) M.-L. Ma, J.-H. Qin, C. Ji, H. Xu, R. Wang, B.-J. Li, S.-Q. Zang, H.-W. Hou and S. R. Batten, *J. Mater. Chem. C.*, 2014, **2**, 1085; (i) X.-Z. Song, S.-Y. Song, M. Zhu, Z.-M. Hao, X. Meng, S.-N. Zhao and H.-J. Zhang, *Dalton Trans.*, 2013, **42**, 13231.
- (a) R. J. Hill, D. L. Long, N. R. Champness, P. Hubberstey and M. Schröder, *Acc. Chem. Res.*, 2005, **38**, 337; (b) N. W. Ockwig, O. D. Friedrichs, M. I. O'Keeffe and O. M. Yaghi, *Acc. Chem. Res.*, 2005, **38**, 176; (c) H.-L. Jiang, T. A. Makal and H.-C. Zhou, *Coord. Chem. Rev.*, 2013, **257**, 2232.
- (a) A. Phan, C. J. Doonan, F. J. Uribe-Romo, C. B. Knobler, M. O'Keeffe and O. M. Yaghi, *Acc. Chem. Res.*, 2010, **43**, 58; (b) J. P. Zhang, Y. B. Zhang, J. B. Lin and X. M. Chen, *Chem. Rev.*, 2012, **112**, 1001; (c) D.-S. Li, Y.-P. Wu, J. Zhao, J. Zhang and J. Y. Lu, *Coord. Chem. Rev.*, 2014, **261**, 1; (d) F. Wang, Y. X. Tan, H. Yang, H. X. Zhang, Y. Kang and J. Zhang, *Chem. Commun.*, 2011, **47**, 5828.
- (a) L. Carlucci, G. Ciani and D. M. Proserpio, *Coord. Chem. Rev.*, 2003, **246**, 247; (b) J. Yang, J.-F. Ma, S. R. Batten, S. W. Ng and Y.-Y. Liu, *CrystEngComm*, 2011, **13**, 5296; (c) J. Xu, Z.-S. Bai, M.-S. Chen, Z. Su, S.-S. Chen and W.-Y. Sun, *CrystEngComm*, 2009, **11**, 2728; (d) Y. Mu, G. Han, S. Ji, H. Hou and Y. Fan, *CrystEngComm*, 2011, **13**, 5943.
- (a) J. H. Park, W. R. Lee, Y. Kim, H. J. Lee, D. W. Ryu, W. J. Phang and C. S. Hong, *Cryst. Growth Des.*, 2014, **14**, 699; (b) H.-L. Jiang, Y. Tatsu, Z.-H. Lu and Q. Xu, *J. Am. Chem. Soc.*, 2010, **132**, 5586; (c) H. He, D. Yuan, H. Ma, D. Sun, G. Zhang and H.-C. Zhou, *Inorg. Chem.*, 2010, **49**, 7605.
- (a) L.-P. Xue, X.-H. Chang, S.-H. Li, L.-F. Ma and L.-Y. Wang, *Dalton Trans.*, 2014, **43**, 7219; (b) Y. Liu, Y. Qi, Y.-H. Su, F.-H. Zhao, Y.-X. Che and J.-M. Zheng, *CrystEngComm*, 2010, **12**, 3283; (c) G.-H. Cui, J.-R. Li, J.-L. Tian, X.-H. Bu and S. R. Batten, *Cryst. Growth Des.*, 2005, **5**, 1775; (d) Y. Qi, F. Luo, S. R. Batten, Y.-X. Che and J.-M. Zheng, *Cryst. Growth Des.*, 2008, **8**, 2806; (e) L.-F. Ma, M.-L. Han, J.-H. Qin, L.-Y. Wang and M. Du, *Inorg. Chem.*, 2012, **51**, 9431; (f) Y.-P. Wu, D.-S. Li, J. Zhao, Z.-F. Fang, W.-W. Dong, G.-P. Yang and Y.-Y. Wang, *CrystEngComm*, 2012, **14**, 4745; (g) A. G. Wong-Foy, O. Lebel and A. J. Matzger, *J. Am. Chem. Soc.*, 2007, **129**, 15740; (h) C. S. Lim, J. K. Schnobrich, A. G. Wong-Foy and A. J. Matzger, *Inorg. Chem.*, 2010, **49**, 5271; (i) B. Li, F. Yang, Y. Zhang, G. Li, Q. Zhou, J. Hua, Z. Shi and S. Feng, *Dalton Trans.*, 2012, **41**, 2677; (j) D. Sun, M.-Z. Xu, S.-S. Liu, S. Yuan, H.-F. Lu, S.-Y. Feng and D.-F. Sun, *Dalton Trans.*, 2013, **42**, 12324.
- (a) F. Guo, F. Wang, H. Yang, X. Zhang and J. Zhang, *Inorg. Chem.*, 2012, **51**, 9677; (b) J.-Q. Liu, Y.-Y. Wang, T. Wu and J. Wu, *CrystEngComm*, 2012, **14**, 2906; (c) J.-H. Qin, L.-F. Ma, Y. Hu and L.-Y. Wang, *CrystEngComm*, 2012, **14**, 2891; (d) J.-Q. Liu, Y.-S. Huang, Y.-Y. Zhao and Z.-B. Jia, *Cryst. Growth Des.*, 2011, **11**, 569; (e) Y.-L. Liu, K.-F. Yue, D.-S. Li, Y. Yu, L. Hou and Y.-Y. Wang, *CrystEngComm*, 2013, **15**, 2791; (f) H.-J. Hao, F.-J. Liu, H.-F. Su, Z.-H. Wang, D.-F. Wang, R.-B. Huang and L.-S. Zheng, *CrystEngComm*, 2012, **14**, 6726; (g) D. Sun, S. Yuan, H. Wang, H.-F. Lu, S.-Y. Feng and D.-F. Sun, *Chem. Commun.*, 2013, **49**, 6152; (h) Z.-H. Yan, L.-L. Han, Y.-Q. Zhao, X.-Y. Li, X.-P. Wang, L. Wang and D. Sun, *CrystEngComm*, 2014, **16**, 8747.
- (a) L. Zhou, C. Wang, X. Zheng, Z. Tian, L. Wen, H. Qua and D. Li, *Dalton Trans.*, 2013, **42**, 16375; (b) F. Kettner, C. Worch, J. Moellmer, R. Gläser, R. Staudt and H. Krautscheid, *Inorg. Chem.*, 2013, **52**, 8738; (c) X. Chen, A. M. Plonka, D. Banerjee and J. B. Parise, *Cryst. Growth Des.*, 2013, **13**, 326; (d) Q. Chen, P.-C. Guo, S.-P. Zhao, J.-L. Liu and X.-M. Ren, *CrystEngComm*, 2013, **15**, 1264;

- (e) H.-H. Zou, Y.-P. He, L.-C. Gui and F.-P. Liang, *CrystEngComm*, 2011, **13**, 3325; (f) J. Zhang, S. Chen, T. Wu, P. Feng and X. Bu, *J. Am. Chem. Soc.*, 2008, **130**, 12882.
- 10 X.-Y. Huang, K.-F. Yue, J.-C. Jin, J.-Q. Liu, C.-J. Wang, Y.-Y. Wang
5 and Q.-Z. Shi, *Inorg. Chem. Commun.*, 2010, **13**, 338.
- 11 G. M. Sheldrick, *SADABS, Program for Siemens Area Detector
Absorption Corrections*, University of Göttingen, Germany, 1997.
- 12 (a) G.M. Sheldrick, SHELXTL Version 5.1. Bruker Analytical X-ray
10 Instruments Inc., Madison, Wisconsin, USA, 1998; (b) G. M. Sheldrick, SHELXL-97, *Program for the Refinement of Crystal
Structure*; University of Göttingen, Germany, 1997.
- 13 (a) R. G. Goel and A. L. Beauchamp, *Inorg. Chem.*, 1983, **22**, 395;
(b) T. Li, H. Zhou, P. Lin and S.-W. Du, *Inorg. Chem. Commun.*,
2006, **9**, 1263.
- 15 14 (a) see website: <<http://rcsr.anu.edu.au/>>; (b) V. A. Blatov, L.
Carlucci, G. Ciani and D. M. Proserpio, *CrystEngComm*, 2004, **6**,
378; (c) X.-M. Liu, L.-H. Xie, J.-B. Lin, R.-B. Lin, J.-P. Zhang and
X.-M. Chen, *Dalton Trans.*, 2011, **40**, 8549; (d) F.-H. Zhao, Y.-X.
Che and J.-M. Zheng, *Inorg. Chem. Commun.*, 2012, **24**, 200; (e) S.-
20 S. Chen, Z.-S. Bai, J. Fan, G.-C. Lv, Z. Su, M.-S. Chen and W.-Y.
Sun, *CrystEngComm*, 2010, **12**, 3091.
- 15 (a) I. A. Baburin, V. A. Blatov, L. Carlucci, G. Ciani and D. M.
Proserpio, *Cryst. Growth. Des.*, 2008, **8**, 519; (b) A. Westcott, N.
Whitford and M. J. Hardie, *Inorg. Chem.*, 2004, **43**, 3663; (c) Z. F.
25 Chen, R. G. Xiong, B. F. Abrahams, X. Z. You and C. M. Che,
Dalton Trans., 2001, 2453.
- 16 S. Z. Zhan, M. Li, X. P. Zhou, J. H. Wang, J. R. Yang and D. Li,
Chem. Commun., 2011, **47**, 12441.
- 17 (a) Y. Gong, Z. Hao, J. L. Sun, H.-F. Shi, P.-G. Jiang and J.-H. Lin,
30 *Dalton Trans.*, 2013, **42**, 13241; (b) H.-J. Hao, F.-J. Liu, H.-F. Su, Z.-
H. Wang, D.-F. Wang, R.-B. Huang and L.-S. Zheng,
CrystEngComm, 2012, **14**, 6726; (c) X.-Y. Huang, K.-F. Yue, J.-C.
Jin, J.-Q. Liu, C.-J. Wang, Y.-Y. Wang and Q.-Z. Shi, *Inorg. Chem.
Commun.*, 2010, **13**, 338.
- 35 18 (a) W. Chen, J.-Y. Wang, C. Chen, Q. Yue, H.-M. Yuan, J.-S. Chen
and S.-N. Wang, *Inorg. Chem.*, 2003, **42**, 944; (b) Z.-H. Li, L.-P.
Xue, S.-H. Li, J.-G. Wang, B.-T. Zhao, J. Kan and W.-P. Su
CrystEngComm, 2013, **15**, 2745; (c) X.-Q. Fang, Z.-P. Deng, L.-H.
Huo, W. Wan, Z.-B. Zhu, H. Zhao and S. Gao, *Inorg. Chem.*, 2011,
40 **50**, 12562; (d) D. Sun, Z.-H. Yan, M. Liu, H. Xie, S. Yuan, H. Lu, S.
Feng and D. Sun, *Cryst. Growth Des.*, 2012, **12**, 2902.